

## Zeolites

## Organotemplate-Free Synthesis of a High-Silica Zeolite with a TON Structure in the Absence of Zeolite Seeds

Yeqing Wang,<sup>[a]</sup> Chenqi Zhu,<sup>[a]</sup> Jing Qiu,<sup>[a]</sup> Fan Jiang,<sup>[a]</sup> Xiangju Meng,<sup>\*[a]</sup> Xiong Wang,<sup>[a]</sup> Chi Lei,<sup>[a]</sup> Yinying Jin,<sup>[a]</sup> Shuxiang Pan,<sup>[a]</sup> and Feng-Shou Xiao<sup>\*[a]</sup>

**Abstract:** A high-silica zeolite with a TON structure designated as ZJM-4 was successfully synthesized in the absence of any organic templates and zeolite seeds. Many factors such as the SiO<sub>2</sub>/K<sub>2</sub>O ratio, Si/Al ratio, SiO<sub>2</sub>/H<sub>2</sub>O in the starting aluminosilicate gels, crystallization temperature, and crystallization time strongly influence the formation of the ZJM-4 zeolite. Interest-

ingly, this synthesis shows very efficient silica utilization in the starting gels (>80 %). Catalytic tests on the isomerization of *m*-xylene to *p*-xylene show that the ZJM-4 catalyst has high selectivity to *p*-xylene (ca. 80 %), which could be potentially important for industrial applications for the ZJM-4 zeolite as a candidate catalyst in the future.

## Introduction

Zeolites have unique porosity and high surface area, playing important roles in ion exchange, catalysis, adsorption, and separation. The high-silica zeolite with a TON structure, with a one-dimensional 10-membered ring pore system with medium-sized pores of ca. 0.47 × 0.55 nm,<sup>[1,2]</sup> has been widely applied in catalytic conversions such as isomerization,<sup>[3–7]</sup> paraffin hydroconversion,<sup>[8]</sup> and propene trimerization.<sup>[9]</sup> Notably, the high-silica zeolite with a TON structure such as ZSM-22 is synthesized in the presence of organic templates.<sup>[10]</sup> The use of organic templates not only increases the synthesis cost but also produces polluted wastes, which strongly limit its practical applications in the industrial processes. Therefore, low-cost and environmentally friendly synthesis of ZSM-22 is highly desirable.<sup>[11,12]</sup>

Recently, it has been reported that seed-directed synthesis is a generalized route for the synthesis of zeolites in the absence of organic templates. The first example is the synthesis of Beta zeolite,<sup>[13]</sup> followed by syntheses such as FER,<sup>[14]</sup> RTH,<sup>[15]</sup> and MTT.<sup>[16]</sup> More recently, Wang et al. reported a successful seed-directed synthesis of high-silica ZSM-22 zeolite in the absence of organic templates, which was designated as ZJM-4.<sup>[17]</sup> This route significantly reduces the ZSM-22 zeolite cost and polluted wastes in the synthesis, but it is worth noting that the synthesis of ZSM-22 zeolite seeds still requires organic templates. In other words, the organic templates cannot be entirely avoided in the synthesis of the ZJM-4 zeolite.

On the other hand, it is interesting to note that many industrially used zeolites are completely synthesized in the absence of organic templates such as ZSM-5, Y, and A. Besides their unique structural features, low-cost and organotemplate-free syntheses are also important factors for the wide applications in the industrial processes. Currently, it is a challenge to produce a complete organotemplate-free synthesis of ZJM-4 zeolite in the absence of ZSM-22 zeolite seeds.

Structural analyses of ZSM-22 and ZSM-5 zeolites show that both zeolites have similar zeolite building units, and a key factor for the synthesis of the ZSM-5 zeolite in the absence of organic templates is to induce the formation of zeolite building units.<sup>[18]</sup> Inspired by the organotemplate-free synthesis of ZSM-5 zeolite, we have carefully adjusted the composition of the starting gels to be favorable for the formation of the zeolite building units of the TON structure in the absence of any organic templates. When the crystallization time is long enough, high silica zeolite with a TON structure could be successfully synthesized in the absence of any organic templates.

Herein, we have demonstrated an organotemplate-free synthesis of ZJM-4 zeolite in the absence of ZSM-22 zeolite seeds by adjusting the composition of the starting gels. The ZJM-4 zeolite has high crystallinity and similar textural parameters to those of ZSM-22 synthesized in the presence of organic templates. More importantly, the synthesis of the ZJM-4 zeolite has very high silica utilization.

## Results and Discussion

## Organotemplate-Free Synthesis of the ZJM-4 Zeolite in the Absence of the Zeolite Seeds

Figure 1 shows the XRD pattern and SEM image of the as-synthesized ZJM-4 zeolite as well as the Ar sorption isotherms of H-ZJM-4. The sample XRD pattern (Figure 1, a) shows a series

[a] Department of Chemistry, Zhejiang University  
Hangzhou 310028, P. R. China  
E-mail: mengxj@zju.edu.cn  
fsxiao@zju.edu.cn

<http://www.chem.zju.edu.cn/xiaofs/News/News.html>

Supporting information for this article is available on the WWW under <http://dx.doi.org/10.1002/ejic.201501223>.

of characteristic peaks associated with the TON structure.<sup>[19,20]</sup> The sample SEM image (Figure 1, b) exhibits pure and very uniform rod-like crystals with a length of 2–3  $\mu\text{m}$ , in good agreement with the typical morphology of aluminosilicate zeolites with a TON structure, reported previously.<sup>[10]</sup> The sample Ar sorption isotherms (Figure 1, c) exhibit a steep increase in the curve at a relative pressure of  $10^{-6} < P/P_0 < 0.01$ , which is characteristic of Langmuir adsorption from the filling of the micropores. The HK pore size distribution is estimated at 0.55 nm. The BET surface area and micropore volume are 171  $\text{m}^2/\text{g}$  and 0.066  $\text{cm}^3/\text{g}$ , respectively. These values are consistent with those of the ZSM-22 zeolite synthesized in the presence of diaminoctane.<sup>[21]</sup>

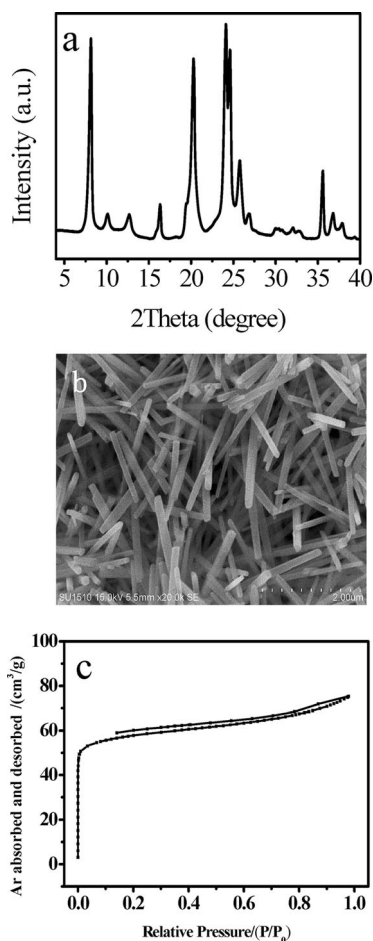


Figure 1. (a) XRD pattern and (b) SEM image of the as-synthesized ZJM-4 sample as well as (c) Argon sorption isotherms of the H-ZJM-4 sample.

Figure 2 shows the  $^{27}\text{Al}$  NMR spectra of the as-synthesized and calcined ZJM-4 zeolite and the  $^{29}\text{Si}$  MAS NMR spectrum of the as-synthesized ZJM-4 zeolite. In Figure 2 (A), the samples exhibit one strong peak at  $\delta = 57.5$  ppm, which corresponds with the tetrahedral coordination aluminum in the framework of the ZJM-4 zeolite.<sup>[22]</sup> The absence of the signal at ca. 0 ppm confirms that all aluminum atoms in the samples are tetrahedrally located in the zeolite framework. After calcination at 550  $^{\circ}\text{C}$  for 5 h, we still do not observe the signal at ca. 0 ppm in the ZJM-4 sample, indicating that these aluminum species in the framework are quite thermally stable, which is important

for industrial applications. As shown in Figure 2 (B), the three major peaks at about  $-111$ ,  $-113$ , and  $-115$  ppm are assigned to the Si(4Si) species. The peak at  $-104.5$  ppm is assigned to Si(3Si,1Al) and/or Si(3Si,1OH). These results indicate that most of the silicon atoms in the ZJM-4 zeolite are Si(4Si) species.

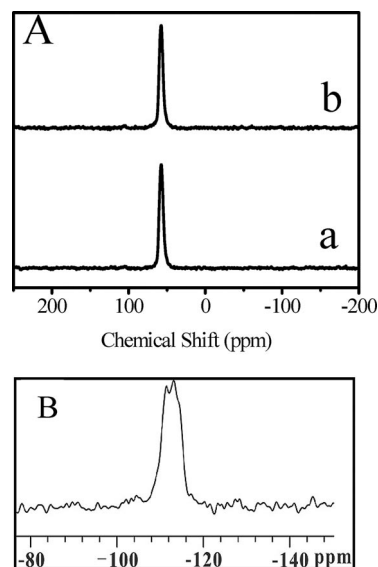


Figure 2. (A)  $^{27}\text{Al}$  MAS NMR spectra of the (a) as-synthesized and (b) calcined ZJM-4 sample and the (B)  $^{29}\text{Si}$  MAS NMR spectrum of the as-synthesized ZJM-4 zeolite.

The Si/Al ratio of the ZJM-4 was analyzed by inductively coupled plasma (ICP) as 41 (Table S3). It is worth mentioning that the silica utilization in the organotemplate-free synthesis of the ZJM-4 zeolite is over 80%. Normally, the organotemplate-free and seed-directed synthesis of zeolites such as Beta (30–40%) have relatively low silica utilization.<sup>[23]</sup> Obviously, the high silica utilization in the organotemplate-free synthesis in the absence of zeolite seeds should be potentially important for industrial applications of this ZJM-4 zeolite.

### The Factors for Organotemplate-Free Synthesis of the ZJM-4 Zeolite in the Absence of Zeolite Seeds.

Figures 3 and 4 show XRD patterns and SEM images of the samples synthesized under various conditions, respectively, as presented in Tables S1 and S2. Clearly, the amount of KOH added to the starting gels significantly influences the formation of the ZJM-4 zeolite. When the ratio of  $\text{SiO}_2/\text{K}_2\text{O}$  is 14.29, amorphous product is obtained (parts a in Figures 3 and 4, and Run 1 in Table S1); When the  $\text{SiO}_2/\text{K}_2\text{O}$  ratio is decreased to 12.84, the product contains a little of the amorphous phase (parts b in Figures 3 and 4 and Run 2 in Table S1); When the  $\text{SiO}_2/\text{K}_2\text{O}$  ratio is reduced to 11.88, a pure phase of ZJM-4 zeolite is obtained (Figure 1, a and b, and Run 3 in Table S1); When the  $\text{SiO}_2/\text{K}_2\text{O}$  ratios are below 10, the product consists of cristobalite (Figure 3, d, Figure 4, c and d, and Runs 4 and 5 in Table S1). Hence, the ratios of  $\text{K}_2\text{O}/\text{SiO}_2$  play an important role in obtaining the pure phase of the ZJM-4 zeolite, which should be carefully adjusted.

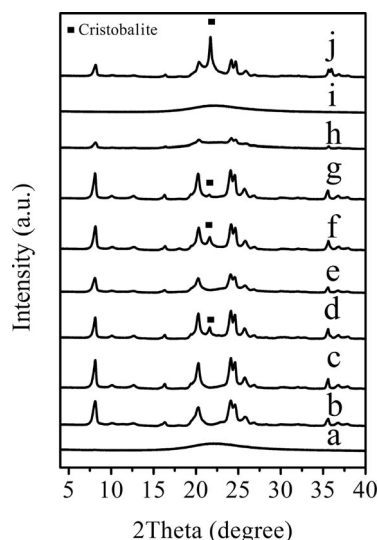


Figure 3. XRD patterns of the ZJM-4 samples synthesized under various conditions. The  $\text{SiO}_2/\text{K}_2\text{O}$  ratios of (a) 14.29, (b) 12.84, (c) 11.88, and (d) 8.33 under a temperature of 150 °C, a Si/Al ratio of 50, and  $\text{SiO}_2/\text{H}_2\text{O}$  ratio of 0.0225; the Si/Al ratios of (e) 40 and (f) 75 under a temperature of 150 °C, a  $\text{SiO}_2/\text{K}_2\text{O}$  ratio of 11.88, and  $\text{SiO}_2/\text{H}_2\text{O}$  ratio of 0.0225;  $\text{SiO}_2/\text{H}_2\text{O}$  ratio of (g) 0.0667 and (h) 0.0200 under a temperature of 150 °C, a Si/Al ratio of 50, and  $\text{SiO}_2/\text{K}_2\text{O}$  ratio of 11.88; a temperature of (i) 135 °C and (j) 165 °C, a  $\text{SiO}_2/\text{K}_2\text{O}$  ratio of 11.88, Si/Al ratio of 50, and  $\text{SiO}_2/\text{H}_2\text{O}$  ratio of 0.0225.

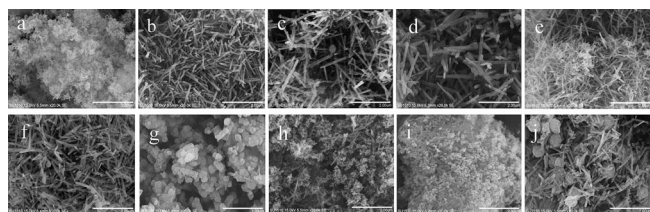


Figure 4. SEM images of the ZJM-4 samples synthesized under various conditions. The  $\text{SiO}_2/\text{K}_2\text{O}$  ratio of (a) 14.29, (b) 12.84, (c) 10.00, and (d) 8.33 under a temperature of 150 °C, a Si/Al ratio of 50, and  $\text{SiO}_2/\text{H}_2\text{O}$  ratio of 0.0225; the Si/Al ratios of (e) 40 and (f) 75 under a temperature of 150 °C, a  $\text{SiO}_2/\text{K}_2\text{O}$  ratio of 11.88, and  $\text{SiO}_2/\text{H}_2\text{O}$  ratio of 0.0225; the  $\text{SiO}_2/\text{H}_2\text{O}$  of (g) 0.0667 and (h) 0.0200 under a temperature of 150 °C, a Si/Al ratio of 50, and  $\text{SiO}_2/\text{K}_2\text{O}$  of 11.88; a temperature of (i) 135 °C and (j) 165 °C, a  $\text{SiO}_2/\text{K}_2\text{O}$  ratio of 11.88, Si/Al ratio of 50, and  $\text{SiO}_2/\text{H}_2\text{O}$  ratio of 0.0225 (scale bar: 2  $\mu\text{m}$ ).

In addition, the ratios of Si/Al in the starting aluminosilicate gels also influence the purity of the ZJM-4 zeolite. For example, when the Si/Al ratio in the starting gel is 25, it is always an amorphous phase (Run 6 in Table S1); when the Si/Al ratios in the starting gel reaches 40, the major product is the ZJM-4 zeolite together with a small amount of the amorphous phase (parts e in Figures 3 and 4, and Run 7 in Table S1); when the Si/Al ratio in the starting gel reaches 50, pure ZJM-4 zeolite can be obtained; when the Si/Al ratios are over 60 (parts f in Figures 3 and 4, and Runs 8 and 9 in Table S1) an impurity of cristobalite can be obtained.

Furthermore, it is observed that the ratios of  $\text{SiO}_2/\text{H}_2\text{O}$  should be carefully adjusted. The suitable ratio is 0.0225. Too few or too much water in the starting gels always results in the impurity of cristobalite (parts g in Figures 3 and 4, and Runs 10 and 11 in Table S1) or the amorphous phase (parts h in Figures 3 and 4, and Runs 12 and 13 in Table S1).

The crystallization temperature in the synthesis is also an important factor for obtaining the pure phase of the ZJM-4 zeolite. The products only consist of the amorphous phase when the temperature is 135 °C (parts i in Figures 3 and 4, and Run 14 in Table S1); when the temperature is increased to 150 °C, a pure phase of the ZJM-4 zeolite is obtained (Run 3 in Table S1); when the temperature is 165 °C, an impurity of cristobalite is formed in the final product (parts j in Figures 3 and 4, and Run 15 in Table S1).

The rotation crystallization is also necessary for the organo-template-free synthesis of the ZJM-4 zeolite. When the sample is crystallized under static conditions all of the products are amorphous (Run 16 in Table S1). These results suggest that the rotation conditions are favorable for the nucleation and crystallization of the ZJM-4 zeolite.

Besides, the crystallization time influence the synthesis of the ZJM-4 zeolite. When the crystallization time is less than 26 h, the major product is amorphous  $\text{SiO}_2$  (Run 1 in Table S2). When the crystallization time reaches 60 h, a small amount of cristobalite occurs in the products (Run 3 in Table S2).

As presented in Tables S1 and S2, it is apparent that many factors such as the  $\text{SiO}_2/\text{K}_2\text{O}$  ratio, Si/Al ratio,  $\text{SiO}_2/\text{H}_2\text{O}$  in the starting aluminosilicate gels, crystallization temperature, and crystallization time influence the synthesis of the ZJM-4 zeolite. The pure ZJM-4 zeolite could only be obtained in a narrow phase diagram of  $\text{K}_2\text{O}-\text{Al}_2\text{O}_3-\text{SiO}_2-\text{H}_2\text{O}$  by a comprehensive consideration of these factors.

### Importance of Starting Composition Adjustment for the Synthesis of the ZJM-4 Zeolite

It has been reported that the zeolite building units play an important role in the formation of the zeolite structure.<sup>[24,25]</sup> Therefore, in this work, it is proposed to form the zeolite building units to induce the crystallization of the ZJM-4 zeolite. Figure 5 (a) shows the IR spectrum obtained from the suitable molar ratio of the starting gels for the synthesis of the ZJM-4, giving a weak band at about 554  $\text{cm}^{-1}$  associated with the asymmetric mode of five rings in the zeolite building units, which is consistent with that (551  $\text{cm}^{-1}$ ) of the ZJM-4 zeolite (Figure 5, b).<sup>[26,27]</sup> This result suggests that the starting aluminosilicate

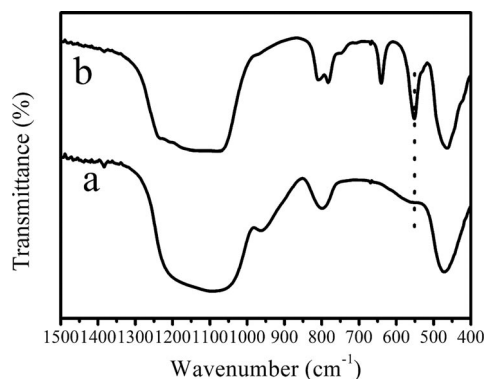


Figure 5. FTIR spectra of (a) the starting gel for the synthesis of the ZJM-4 zeolite with a molar ratio of 0.01  $\text{Al}_2\text{O}_3/1.0 \text{SiO}_2/0.084 \text{K}_2\text{O}/45 \text{H}_2\text{O}$  and the (b) as-synthesized ZJM-4 zeolite.

silicate gel already contained the TON building units. These building units are possibly favorable for the crystallization of the ZJM-4 zeolite. In contrast, when these building units are absent in the starting gels, it is difficult to obtain the ZJM-4 crystals. After crystallization of the ZJM-4 zeolite, along with new bands at 808 and 640  $\text{cm}^{-1}$  the band at 551  $\text{cm}^{-1}$  becomes very strong (Figure 5, b). These bands are typically characteristic of zeolite ZJM-4 with a TON zeolite structure. These results confirm the importance of the zeolite building units in the starting gels for the formation of the ZJM-4 zeolite.

### Catalytic Tests of ZJM-4

The acid strength of the H-ZJM-4 zeolite has been characterized by  $\text{NH}_3$ -TPD (Figure 6), giving two peaks centered at 221 and 450  $^\circ\text{C}$ , which are assigned to relatively weak and strong acidic sites in the sample. The quantitative estimation of this curve shows that the concentration of the weak and strong acidic sites is 0.33 and 0.38 mmol/g, respectively. These results indicate that the H-form of the ZJM-4 zeolite has both strong and weak acidic sites, which are very similar to those of conventional zeolites with a TON structure.

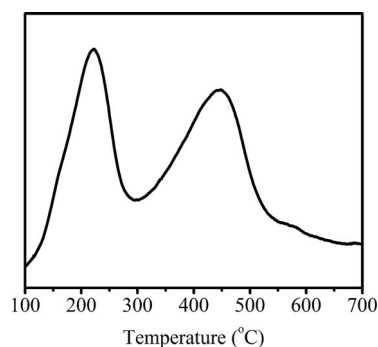


Figure 6.  $\text{NH}_3$ -TPD curve of the H-ZJM-4 zeolite.

Figure 7 presents catalytic data from the *m*-xylene isomerization over the H-ZJM-4 zeolite. The H-ZJM-4 exhibits excellent selectivity to *p*-xylene (ca. 80%). This value is comparable with that of the H-ZJM-4 zeolite synthesized from seed-directed and organotemplate-free conditions.<sup>[17]</sup> Considering the complete avoidance of organic templates and efficient silica utilization in

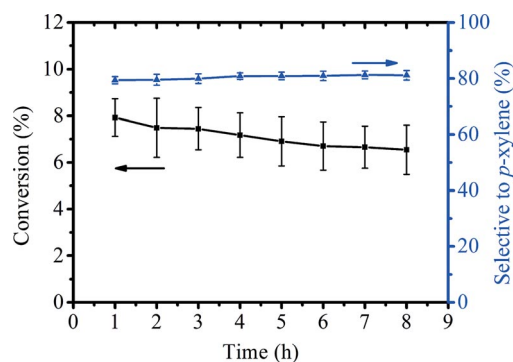


Figure 7. Catalytic (■) conversion of *m*-xylene and (▲) selectivity for *p*-xylene in *m*-xylene isomerization over the H-ZJM-4 zeolite catalyst.

the synthesis, the excellent selectivity is potentially important for catalytic applications of low-cost ZJM-4 zeolite in the future.

### Conclusions

In summary, ZJM-4 zeolite with a TON structure has been successfully synthesized under organotemplate-free and seed-free conditions. This route has efficient silica utilization, which is of great significance for reduction of polluted wastes and zeolite cost. The ZJM-4 zeolite has a stable tetrahedral aluminum species and strong acidic sites, which is important for catalytic applications in the future.

### Experimental Section

**Materials:** Potassium hydroxide (KOH) was purchased from Sino-pharm Chemical Reagent Co. Ltd. Tetraethyl orthosilicate (TEOS) and aluminum sulfate  $[\text{Al}_2(\text{SO}_4)_3 \cdot 18\text{H}_2\text{O}]$  were purchased from Chinasun Specialty Products Co. Ltd. Ammonium nitrate was purchased from the Chengdu Kelong Chemical Reagent Factory. *m*-Xylene was obtained from the Aladdin Chemical Reagent Company.

**Materials Synthesis:** ZJM-4 zeolite was hydrothermally synthesized from the starting gels with molar ratios of 0.0067–0.02  $\text{Al}_2\text{O}_3/1.0 \text{SiO}_2/0.07\text{--}0.12 \text{K}_2\text{O}/15\text{--}55 \text{H}_2\text{O}$  in a poly-(tetrafluoroethylene)-lined stainless steel autoclave dynamically (50 rpm) at a temperature of 135–165  $^\circ\text{C}$  for 0–60 h. As a typical run for the synthesis of ZJM-4 in the absence of organic templates and the zeolite seeds, KOH (0.16 g) and  $\text{Al}_2(\text{SO}_4)_3 \cdot 18\text{H}_2\text{O}$  (0.096 g) were dissolved in deionized water (11.5 g), followed by the addition of TEOS (3.0 g). After stirring for 4 h, the mixture was transferred into a Teflon<sup>®</sup>-lined autoclave oven and crystallized at 150  $^\circ\text{C}$  for 48 h under rotation conditions (50 rpm). Finally, the product was collected by filtration, washed with deionized water, and dried at 100  $^\circ\text{C}$  for 6 h.

The H-form of the ZJM-4 zeolite was obtained by ion-exchange with a  $\text{NH}_4\text{NO}_3$  solution (1 M) at 80  $^\circ\text{C}$  for 1 h (1 g of ZJM-4 zeolite in 50 mL of solution), which was performed three times. The ion-exchanged ZJM-4 zeolite was heated to 550  $^\circ\text{C}$  at a heating rate of 1  $^\circ\text{C}/\text{min}^{-1}$  and kept at 550  $^\circ\text{C}$  for 5 h in flowing  $\text{O}_2$ . The sample was designated as H-ZJM-4.

**Characterization:** The crystallinity and phase purity of the samples were determined by X-ray powder diffraction (XRD) with a Rigaku Ultimate VI X-ray diffractometer (40 kV, 40 mA) using  $\text{Cu-K}\alpha$  ( $\lambda = 1.5406 \text{ \AA}$ ) radiation from 4 $^\circ$  to 40 $^\circ$  with  $2\theta$ . Scanning electron microscopy (SEM) experiments were performed with Hitachi SU1510 electron microscopes. The Argon sorption isotherms were carried out with a Micromeritics ASAP 2020M and Tristar system. Solid-state  $^{27}\text{Al}$  and  $^{29}\text{Si}$  NMR spectra were recorded with a Varian Infinity plus 400 spectrometer. The sample compositions were determined by inductively coupled plasma (ICP) with a Perkin-Elmer 3300DV emission spectrometer after dissolving the solid products in a hydrofluoric acid solution in a volumetric flask (50 mL). FTIR spectra were recorded with a Thermo Scientific Nicolet iS5 FTIR spectrometer. Temperature-programmed desorption of the  $\text{NH}_3$  (TPD- $\text{NH}_3$ ) curve was carried out with a TCD detector. As a typical run, H-ZJM-4 (200 mg) was placed in a quartz tubular reactor and pretreated at 500  $^\circ\text{C}$  in a nitrogen stream. After cooling to 100  $^\circ\text{C}$ , gaseous  $\text{NH}_3$  was passed through the sample for 30 min. After removal of physically adsorbed  $\text{NH}_3$  by flowing nitrogen for 2 h at 100  $^\circ\text{C}$ , the  $\text{NH}_3$ -TPD curve of the sample was recorded by programmed heating from 100 to 600  $^\circ\text{C}$  with a heating rate of 10  $^\circ\text{C}/\text{min}$ .

Catalytic isomerization of *m*-xylene to *p*-xylene was carried out in a fixed reactor. The zeolite sample (200 mg, 20–40 mesh) was first activated in dry air at 450 °C for 2 h and then cooled to reaction temperature (400 °C) in a flow of dry nitrogen. *m*-Xylene was fed (WHSV = 3 h<sup>-1</sup>) by a metering pump, vaporized in a preheated assembly and then passed through the catalyst. The product was analyzed using on-line gas chromatography (GC1690) with a FID detector.

## Acknowledgments

This work is supported by the National Natural Science Foundation of China (NSFC) (grant numbers 21333009, 21422306 and 91545111), the Fundamental Research Funds for the Central Universities (2015XZZX004-04), and Zhejiang Provincial Natural Science Foundation of China under grant LR15B030001.

**Keywords:** Zeolites · Zeolite building units · Aluminosilicates · Isomerization

- [1] S. Ernst, J. Weitkamp, J. A. Martens, P. A. Jacobs, *Appl. Catal.* **1989**, *48*, 137–148.
- [2] B. Marler, *Zeolites* **1987**, *7*, 393–397.
- [3] J. A. Martens, W. Souverijns, W. H. Verrelst, R. F. Parton, G. F. Froment, P. A. Jacobs, *Angew. Chem. Int. Ed. Engl.* **1995**, *34*, 2528–2530; *Angew. Chem.* **1995**, *107*, 2726–2728.
- [4] R. Byggningsbacka, L.-E. Lindfors, N. Kumar, *Ind. Eng. Chem. Res.* **1997**, *36*, 2990–2995.
- [5] J. Houzviccka, S. Hansildaar, V. Ponec, *J. Catal.* **1997**, *167*, 273–278.
- [6] R. Kumar, P. Ratnasamy, *J. Catal.* **1989**, *116*, 440–448.
- [7] M. A. Asensi, A. Corma, A. Martinez, M. Derewinski, J. Krysciak, S. S. Tamhankar, *Appl. Catal. A* **1998**, *174*, 163–175.
- [8] Th. L. M. Maesen, M. Schenk, T. J. H. Vlugt, J. P. de Jonge, B. Smit, *J. Catal.* **1999**, *188*, 403–412.
- [9] J. A. Martens, W. H. Verrelst, G. Mathys, S. H. Brown, P. A. Jacobs, *Angew. Chem. Int. Ed.* **2005**, *44*, 5687–5690; *Angew. Chem.* **2005**, *117*, 5833–5836.
- [10] F. Di Renzo, F. Renoué, P. Massiani, F. Fajula, F. Figueras, *Zeolite* **1991**, *11*, 539–548.
- [11] X. J. Meng, F.-S. Xiao, *Chem. Rev.* **2014**, *114*, 1521–1543.
- [12] C. S. Cundy, *Chem. Rev.* **2003**, *103*, 663–702.
- [13] B. Xie, J. W. Song, L. M. Ren, Y. Y. Ji, J. X. Li, F.-S. Xiao, *Chem. Mater.* **2008**, *20*, 4533–4535.
- [14] H. Y. Zhang, Q. Guo, L. M. Ren, C. G. Yang, L. F. Zhu, X. J. Meng, C. Li, F.-S. Xiao, *J. Mater. Chem.* **2011**, *21*, 9494–9497.
- [15] T. Yokoi, M. Yoshioka, H. Imai, T. Tatsumi, *Angew. Chem. Int. Ed.* **2009**, *48*, 9884–9887; *Angew. Chem.* **2009**, *121*, 10068.
- [16] Q. M. Wu, X. Wang, X. J. Meng, C. G. Yang, Y. Liu, Y. Y. Jin, Q. Yang, F.-S. Xiao, *Microporous Mesoporous Mater.* **2014**, *186*, 106–112.
- [17] Y. Q. Wang, X. Wang, Q. M. Wu, X. J. Meng, Y. Y. Jin, X. Z. Zhou, F.-S. Xiao, *Catal. Today* **2014**, *226*, 103–108.
- [18] Q. J. Yu, Q. Zhang, J. W. Liu, C. Y. Li, Q. K. Cui, *CrystEngComm* **2013**, *15*, 7680–7687.
- [19] D. Masih, T. Kobayashi, T. Baba, *Chem. Commun.* **2007**, *31*, 3303–3305.
- [20] C. A. Fyfe, G. T. Kokotailo, H. Strobl, C. S. Pasztor, G. Barlow, S. Bradley, *Zeolites* **1989**, *9*, 531–534.
- [21] S. Teketel, W. Skistad, S. Benard, U. Olsbye, K. P. Lillerud, P. Beato, S. Svelle, *ACS Catal.* **2012**, *2*, 26–37.
- [22] M. Derewinski, P. Sarv, A. Mifsud, *Catal. Today* **2006**, *114*, 197–204.
- [23] H. Y. Zhang, B. Xie, X. J. Meng, U. Müller, B. Yilmaz, M. Feyen, S. Maurer, H. Gies, T. Tatsumi, X. H. Bao, W. P. Zhang, D. D. Vos, F.-S. Xiao, *Microporous Mesoporous Mater.* **2013**, *180*, 123–129.
- [24] L. M. Ren, C. J. Li, F. T. Fan, Q. Guo, D. S. Liang, Z. C. Feng, C. Li, S. G. Li, F.-S. Xiao, *Chem. Eur. J.* **2011**, *17*, 6162–6169.
- [25] R. R. Xu, W. Q. Pang, J. H. Yu, Q. S. Huo, J. S. Chen, *Zeolite and Porous Material*, Science Press, Beijing, **2004**.
- [26] W. Mozgawa, *J. Mol. Struct.* **2001**, *596*, 129–137.
- [27] M. B. Park, N. H. Ahn, R. W. Broach, C. P. Nicholas, G. J. Lewis, S. B. Hong, *Chem. Mater.* **2015**, *27*, 1574–1582.

Received: October 24, 2015

Published Online: March 2, 2016